ACS OMEGA

http://pubs.acs.org/journal/acsodf

Article

Light-Induced Anti-Bacterial Effect Against *Staphylococcus aureus* of Porphyrin Covalently Bonded to a Polyethylene Terephthalate Surface

Stefania F. Musolino,[#] Fatima Shatila,[#] Grace M.O. Tieman,[#] Anna C. Masarsky, Matthew C. Thibodeau, Jeremy E. Wulff, and Heather L. Buckley*

Cite This: *ACS Omega* 2022, 7, 29517−29525

Read Online

ACCESS | Metrics & More | Article Recommendations | Supporting Information

ABSTRACT: Antimicrobial photodynamic inactivation represents a promising and potentially greener alternative to conventional antimicrobials, and a solution for multidrug-resistant strains. The current study reports the development and characterization of tetra-substituted diazirine porphyrin covalently bonded to polyethylene terephthalate (PET) and its use as an antimicrobial surface. The diazirine moiety on the porphyrin was activated using a temperature of 120 °C, which initiated a C−H insertion mechanism that irreversibly functionalized the PET surface. Activation of the surface with white LED light in phosphate-buffered saline (PBS) led to singlet oxygen generation, which was detected via the degradation of 9,10-anthracenediylbis(methylene)dimalonic acid (ADMA) over time. The bactericidal effect of the $^1O_2$-producing surface against *Staphylococcus aureus* was determined qualitatively and quantitatively. The growth of the pathogen beneath porphyrin-functionalized PET coupons was reduced; moreover, the PET coupons resulted in a 1.76-log reduction in cell counts after exposure to white LED light for 6 h. This is a promising material and platform for the development of safer antimicrobial surfaces, with applications in healthcare, food packaging, marine surfaces, and other surfaces in the environment.

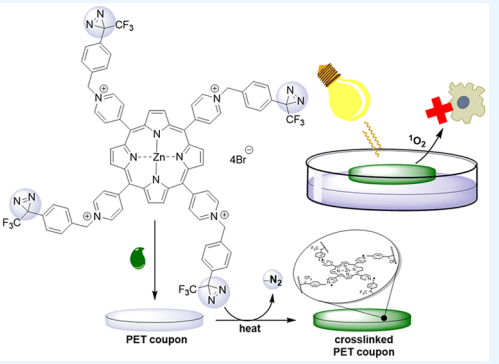

1. INTRODUCTION

Unwanted growth of microorganisms, including bacteria and other potential pathogens, poses a risk to human health due to the variety of infections and diseases they can cause.[1] The growth of pathogenic microorganisms is a global problem in a variety of sectors, including drinking water disinfection, medical settings, and the food industry.[2−5] Current technologies used to combat the issue of bacterial growth include the use of environmentally persistent halogenated cleaners and chlorination technologies that create harmful disinfection byproducts in water treatment.[2,5] Throughout the COVID-19 pandemic, an increase in the disinfection of indoor and outdoor spaces using chlorine or chlorinated disinfectants has resulted in an increase in chlorine concentration in some lakes in China, highlighting the far-reaching environmental impacts of consumer choices of household and industrial cleaners.[6] Another growing concern is the contribution of chlorinated cleaning agents to antibiotic resistance in bacteria.[7] Globally, 700 000 deaths occur due to drug-resistant infections, a number that is expected to increase to 10 million by 2050 in the absence of effective alternatives.[8] The ability of resistant microorganisms to survive on different surfaces facilitates their spread, resulting in hospital-acquired infections (HAI) and foodborne diseases.[9,10] One approach that is being explored is the investigation of the antimicrobial properties of plants that have been traditionally used and prepared by the Indigenous peoples to treat skin infections.[11] Another approach is the development of functionalized antimicrobial surfaces, which have the potential to significantly reduce infections and microbial dissemination and alleviate the problem of discharging antimicrobials into waterways.[12−14] Several approaches involve the design of modified or engineered surfaces. One of the most common strategies is the chemical modification of surfaces through coating or immobilizing photoactive antimicrobials on the polymeric matrix (e.g., nanoparticles, nanofibers, films, and silicon dioxide).[15] For instance, photosensitizers such as rose bengal and methylene blue immobilized on either thin polymeric films of polystyrene or silicon tablets showed great ability to inactivate bacteria.[16,17] Boron-dipyrromethane (BODIPY) derivatives coated on polylactic acid or covalently attached to poly(dimethylsiloxane) kill microbes and eradicate biofilms.[18,19]

Received: July 7, 2022
Accepted: July 28, 2022
Published: August 10, 2022

https://doi.org/10.1021/acsomega.2c04294
ACS Omega 2022, 7, 29517−29525

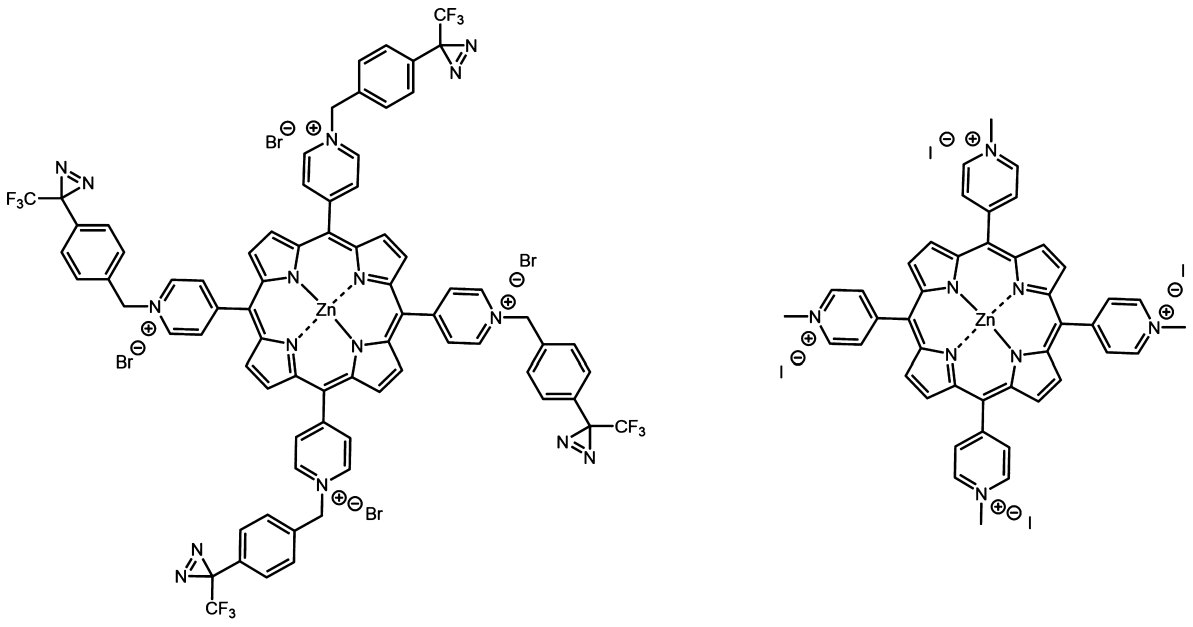

Figure 1. Molecule **1**, zinc(II) 5,10,15,20-tetrakis((*N*-4-[3-(trifluoromethyl)-3*H*-diazirin-3-yl]benzyl)-4-pyridyl)-21*H*,23*H*-porphine tetrabromide, has four possible sites of attachment and can be used to produce singlet oxygen in the presence of light. Molecule **2**, zinc(II) 5,10,15,20-tetrakis(*N*-methyl-4-pyridyl)-21*H*,23*H*-porphine tetraiodide, was used as a control in the cross-linking experiment (section 4.4).

Recent work on cationic polylysine chains grafted on tannic acid showed a switch in antibacterial proprieties and the release of fouling based on pH.[13] Numerous porphyrin derivatives are widely used for the functionalization of materials, as they induce a powerful antimicrobial effect.[20−23]

Functionalizing surfaces using agents with a nonspecific mechanism for microbial inactivation avoids putting selective evolutionary pressure on organisms.[24] A particularly promising method for producing nonspecific antimicrobial activity is the use of photosensitizers to produce singlet oxygen in the presence of light.[25] The singlet oxygen disrupts the cell membrane in a nonselective manner and does not trigger an oxidative stress response, meaning bacteria are not likely to develop a resistance to singlet oxygen.[24,26] At this point, it is debatable whether or not a resistance to singlet oxygen can be developed, but photodynamic inactivation has demonstrated success as an antimicrobial approach.[27,28] There is precedent for using cationic porphyrin molecules, a known group of photosensitizers, in antimicrobial materials.[24,26,29−38] Different physical methods have been applied to incorporate porphyrins and other photosensitizers into surfaces.[26,39−42] Building on previous work by Spontak, where a zinc porphyrin embedded within a polymer effectively inactivated both Gram-negative and Gram-positive bacteria,[26] we designed a zinc porphyrin molecule **1**, zinc(II) 5,10,15,20-tetrakis((*N*-4-[3-(trifluoromethyl)-3*H*-diazirin-3-yl]benzyl)-4-pyridyl)-21*H*,23*H*-porphine tetrabromide, that could be covalently attached to carbon-based polymers (Figure 1). This was achieved through a C−H insertion mechanism wherein diazirine moieties lose dinitrogen after thermal-, photo-, or electro-activation and form a carbon−carbon bond with the substrate. The use of diazirine-based molecules as cross-linkers of aliphatic polymer materials was previously reported by our group.[43,44] Chemical approaches based on the formation of covalent bonds between a photosensitizer and the surface can increase the stability of the material.[39] Additionally, since the porphyrin is covalently attached to a surface, the molecule is prevented from leaching into the environment, meaning that bioaccumulation will not be a concern and it will not be necessary to develop a method for the removal of the molecule. Recently, the use of a tetra-substituted diazirine porphyrin covalently bonded to non-woven melt-blown polypropylene textiles was demonstrated by our group to be efficient for virus inactivation.[45] Here, we explore the use of the diazirine photosensitizer for greener and potentially more effective prevention and treatment of bacteria on polyethylene terephthalate (PET).

2. RESULTS AND DISCUSSION

2.1. Porphyrin and PET. In this study, **1** was cross-linked to PET via a thermally triggered C−H insertion at ∼120 °C. PET was chosen for its thermal stability (melting point of 260 °C).[46] Compound **2** was previously demonstrated to be a photoactivated antimicrobial compound,[26] while molecule **1** was recently reported to successfully inactivate influenza A in our collaborative work.[45]

2.2. Control Experiment. A cross-linking control experiment was performed to further support the porphyrin being cross-linked to the surface (Figure 2).

For the cross-linking control experiment, one of the chosen controls was **2** spin-coated onto a circular PET coupon. Because **2** has no diazirine cross-linker, it should not stay attached to the surface upon rinsing after being heated at 120 °C. The other control was to spin-coat a coupon with **1** but not heat it to 120 °C, thus not activating the diazirine. In the same way as porphyrin **2**, **1** should not stay on the surface upon rinsing if no heat is applied. After rinsing, both controls and a blank were visually compared to a coupon prepared by the standard procedure described in section 4.3. In Figure 2, all the coupons on the right have been rinsed, while all the coupons on the left have not been rinsed. The **2**-treated coupon that was not rinsed was green in color, but was completely clear and looked the same as the blank coupons

https://doi.org/10.1021/acsomega.2c04294
ACS Omega 2022, 7, 29517−29525

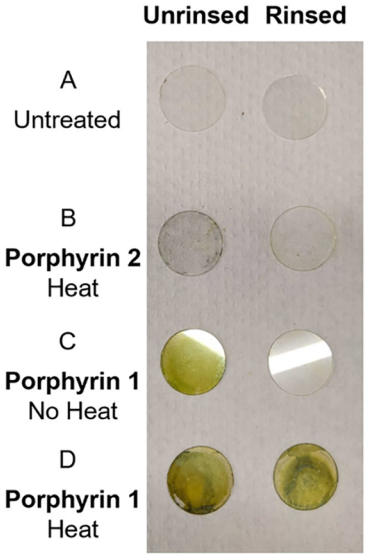

Figure 2. Images from the cross-linking control experiment. The PET coupons in row A had no treatment, the PET coupons in row B were coated with **2** and heated overnight, the PET coupons in row C were coated with **1** and left at room temperature overnight, and the PET coupons in row D were treated as described in section 4.3. Photograph courtesy of G.M.O.T. Copyright 2022.

after being rinsed. Similarly, a representative coupon treated with **1** without the thermal activation of the diazirine groups had a green tinge before it was rinsed, but it was also clear and colorless, and looked the same as the blank coupons after rinsing. When **1** was used and treated with heat, the samples before and after rinsing looked the same, and both had a dark green tinge. This suggests that when a porphyrin with a diazirine is used and heat-treated it does cross-link and does not just become embedded within the surface. If the heat was causing the porphyrin to embed itself within the surface, then **2** would have also remained on the surface after being rinsed. This experiment also shows that heat is required to activate the diazirine, otherwise the non-heat-treated **1** would have been attached to the surface.

2.3. Singlet Oxygen Detection. 9,10-Anthracenediylbis-(methylene)dimalonic acid (ADMA) was chosen as a water-soluble, relatively inexpensive indicator for the selective detection of singlet oxygen.[47] It reacts with singlet oxygen to form a colorless product and does not react with other reactive oxygen species.[47,48] Since the focus of this work is microbial growth prevention via the reaction with singlet oxygen and not other reactive oxygen species, the chosen detector molecule needed to selectively react with singlet oxygen.[47] ADMA was used in previous work as a detector molecule for singlet oxygen produced via the visible-light irradiation of cationic porphyrin molecules.[48]

Figure 3 shows the time series of the absorbance spectra of ADMA solutions exposed to cross-linked **1** in the presence of visible light. The decrease in intensity corresponds to a reduction in the ADMA concentration over the first 24 h, indicating the reaction of ADMA with singlet oxygen. The first noticeable decrease in concentration of ADMA was observed at 15 min, and after 5 h there appeared to be no remaining ADMA.

Using the absorption at 379 nm, ADMA concentrations were compared over 5 h in the presence and absence of both light and porphyrin (Figure 4). The concentration of ADMA is relatively consistent over the 5 h time period for all the experiments except the reaction with ADMA in the light with porphyrin, which fully reacts within 5 h. This further supports that ADMA is degraded as the result of the release of singlet oxygen into the solution as opposed to the porphyrin or the light having an individual effect.

2.4. Antimicrobial Photodynamic Inactivation of *S. aureus*. The current study assessed the bactericidal effect of the cross-linked porphyrin surface against *S. aureus*, a Gram-positive pathogen that is responsible for foodborne illnesses and nosocomial infections.[49] The appearance of multidrug-resistant staphylococcal strains has rendered their treatment more challenging.[50]

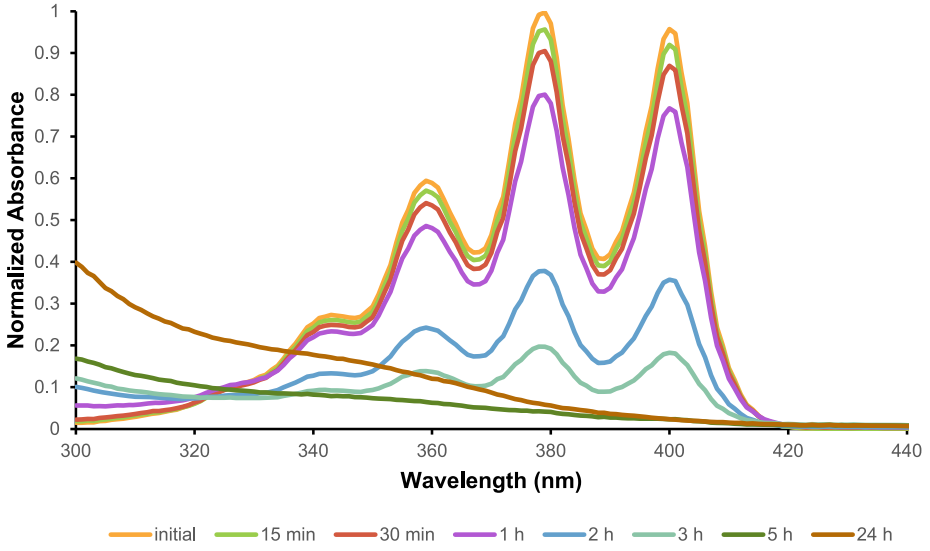

Figure 3. Normalized absorbance measurements of ADMA after being in a PBS solution with PET coupons functionalized with porphyrin **1** for different amounts of time, as described in section 4.5. The initial concentration of ADMA was 0.18 mg/mL. Each replicate was normalized using the maximum absorbance value at λ = 379 nm from the "initial" data set. The absorbance of each solution was measured from 300 to 500 nm at 1 nm intervals.

https://doi.org/10.1021/acsomega.2c04294
ACS Omega 2022, 7, 29517−29525

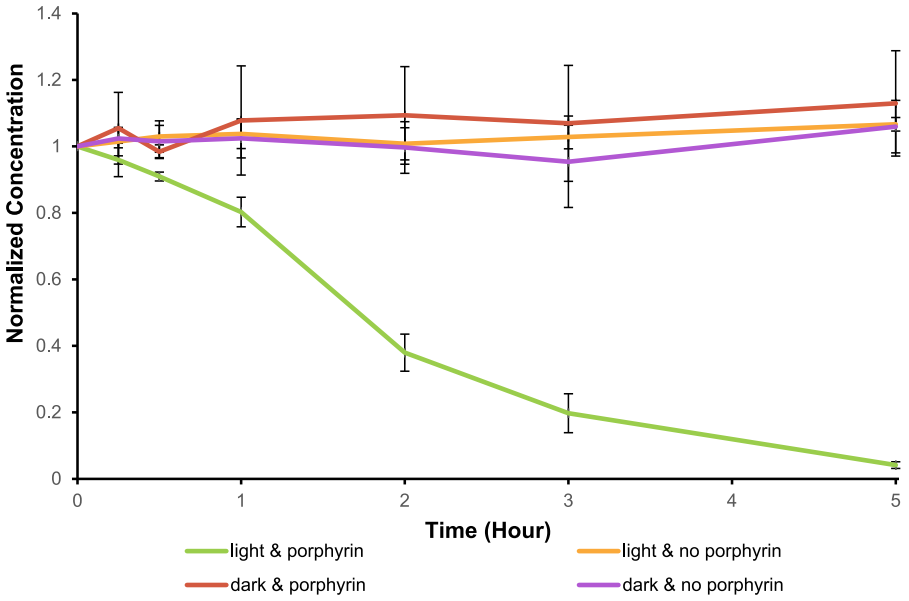

Figure 4. Comparison of the ADMA concentration over time under various conditions. The initial concentration of ADMA was 0.18 mg/mL. Concentrations were calculated for each time point using the absorbance maximum at λ = 379 nm. The concentrations from each experiment were normalized using the initial concentration, and the average (from triplicate measurements) of the concentration for each time point was used. Error bars represent the standard deviation.

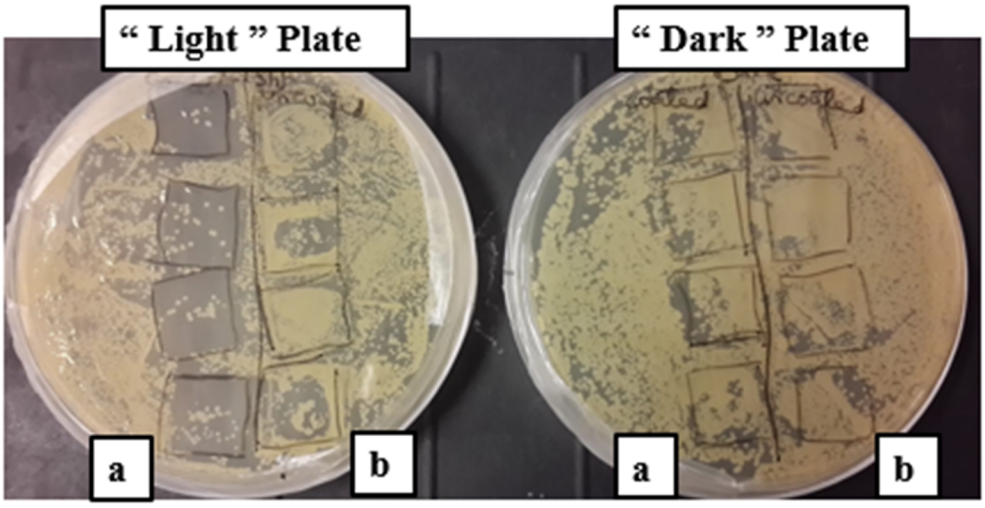

Figure 5. Bactericidal effect of the cross-linked porphyrin surfaces of (a) coated coupons and (b) uncoated coupons, as demonstrated by the reduced *S. aureus* growth beneath the surface, after irradiation with LED light at fluence (26 400 ± 200 lx) for 6 h. The black squares sketched on the covers indicate the positioning of the treated or untreated coupons. Photograph courtesy of F.S. Copyright 2022.

The antibacterial effect against a *S. aureus* strain was assessed quantitatively by determining cell counts and qualitatively by checking the inhibition of bacterial cell growth beneath the surface after irradiation with a white LED light for 6 h (Figure 5). The difference between bacterial cell counts between the light and dark controls was not statistically significant, indicating that neither light alone nor porphyrin alone inhibited bacterial growth. On the other hand, the growth of *S. aureus* in the coated wells of the light plate was significantly reduced, resulting in an approximately 1.76-log reduction (percentage inhibition equivalent to 97.5%).

These results lie within the typical range of inhibition of *S. aureus* growth reported in previous studies that used various materials or surfaces coated with porphyrin photosensitizers. In 2003, Bozja et al. reported the ability of porphyrin-based antimicrobial nylon fibers to inhibit *S. aureus* by 45−95% after exposure to different intensities (10 000 to 60 000 lx) of incandescent light.[51] In 2009, Ringot et al. grafted mesoaryl porphyrin onto cotton fabrics.[52] Only 5% of the bacterial cells in the modified cotton fabric survived being irradiated with white light for 24 h. Similarly, coating cotton fabrics with cationic, anionic, and neutral charged porphyrins inhibited *S. aureus* growth by 100%, 37%, and 93.7%, respectively.[52,53] In 2013, Mbakidi et al. developed porphyrin-coated cellulose papers that resulted in total inhibition after 24 h of irradiation.[54]

Peddinti et al. 2018 developed thermoplastic elastomer films containing zinc tetra(4-*N*-methylpyridyl) porphyrin. Irradiating the coatings for 60 min resulted in percentage inhibitions

https://doi.org/10.1021/acsomega.2c04294
ACS Omega 2022, 7, 29517−29525

equivalent to 99.89% and 99.95% against five different bacterial strains and two viruses.[26]

Previous studies also reported the application of other photosensitizers (methylene blue, toluidine blue, rose bengal, curcumin, quecetin, chlorophyllins, and phenothiazinium) as coatings for different materials. These coatings, which were assessed against *S. aureus*, resulted in 0.35−5-log reductions or percentage inhibitions that ranged from 65% to 99.9% under different illumination conditions.[9,31,55−58]

The antibacterial effect of the coated coupons was also investigated on tryptone soya agar (TSA) plates inoculated with *S. aureus*. The bactericidal effect was determined by comparing the bacterial growth beneath the coated coupons in the "light" plate to that in the "light" and "dark" controls. No inhibition was observed beneath the control coupons in the "light" and "dark" plate. However, the growth beneath the cross-linked porphyrin surface in the light plate was reduced or inhibited when compared to that in the controls (Figure 6).

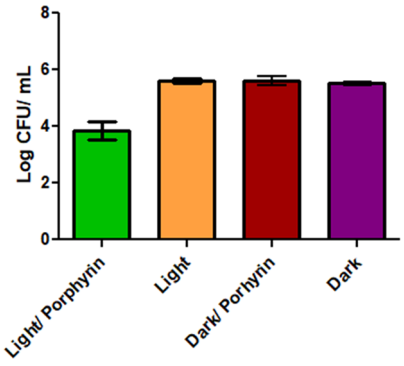

Figure 6. Bactericidal effect of the cross-linked porphyrin surface against *S. aureus*, expressed in log reduction, after irradiation with LED light at 26 400 ± 200 lx for 6 h. Error bars represent the standard deviation.

Similarly, in 2013 and 2015, Merchan et al. and Aluigi et al. demonstrated the ability of porphyrin composite films and methylene blue-doped wool keratin to inhibit *S. aureus* growth being treated with light for 24 h and 75 min, respectively.[57,59]

In 2013, Mbakidi et al. reported that the insoluble nature of the photosensitizer in their work resulted in the formation of reactive oxygen species on the surface of the material.[54] Their diffusion and consequent interaction with target cells damaged the cell envelope. The bactericidal effect of the porphyrin surface can be attributed to the porphyrin-generated singlet oxygen, which can diffuse readily through the relatively porous peptidoglycan layer of Gram-positive bacteria, such as *S. aureus,* and attack (unspecific) vital targets.[12,52]

The degradation of ADMA over time in the presence of cross-linked porphyrin in light supports singlet oxygen production (Figure 4). This chemical assay confirms that the 1.76-log reduction (percentage inhibition equivalent to 97.5%) that occurs only when a porphyrin-functionalized surface is irradiated with visible light (Figure 6) can be attributed to the presence of singlet oxygen in the antibacterial assay of *S. aureus*. This antibacterial effect that occurs for a covalently tethered porphyrin has implications for materials that require long-term stability, which is not possible for a conventional surface coating. It also indicates the capacity to impart similar antimicrobial properties to any polymeric material due to the unique reactivity of the diazirine functionality. Based on these results, this method could lead to a novel method of bacterial growth prevention via the covalent attachment of photodynamic molecules through a diazirine moiety.

3. CONCLUSION

A tetrasubstituted diazirine porphyrin was covalently cross-linked to a PET surface. Through use of ADMA as a detector molecule, singlet oxygen production was confirmed in the presence of the covalently bonded porphyrin and visible LED light. A 1.76-log reduction (97% inhibition) of *S. aureus* after 6 h of irradiation with white LED light was also detected via an antibacterial photodynamic inactivation assay. The confirmation from the ADMA of the presence of singlet oxygen supports the assertion that singlet oxygen is responsible for inactivating *S. aureus*.

This method is a novel way to prevent the growth of bacteria on surfaces through the covalent attachment of antimicrobial molecules. Light activation means the tethered molecules need not be inherently toxic, providing access to potential applications in food packaging, hospital settings, and marine and freshwater contexts. To achieve these applications, next steps include assessing the existing materials with other bacterial species and developing a robust library of diazirine-functionalized antimicrobial molecules appropriate for attachment to diverse materials.

4. METHODS

4.1. Materials. All chemicals were used as received. PET (thickness of 0.254 mm) was purchased from McMaster Carr (8567K92). PET was cut into circular (diameter of 15.6 mm) and square (15.6 × 15.6 mm) coupons. Polystyrene treated 24-well cell culture plates were purchased from VWR (10062-896). ADMA (307554-62-7, ≥ 90%) was purchased from Sigma-Aldrich. Phosphate-buffered saline (PBS) (1×) and methanol (67-56-1, 99%) were purchased from Fischer Scientific (20012043). Luria−Bertani (LB) broth was purchased from Fisher Bioreagents, and tryptone soya agar (TSA) was purchased from Oxoid. A wireless light sensor (701-999, PS-3212) was purchased from PASCO. Absorbance measurements of ADMA were acquired using a Biotek Cytation 5-plate reader. Fluorescence, emission, and absorbance spectra of porphyrin-functionalized PET were acquired using a SpectraMax M5 Multi-Mode Microplate Reader. The synthesis of porphyrin **1** is described in the Supporting Information.

4.2. Light Source and Irradiation Parameters. Unless otherwise indicated, the antimicrobial photodynamic inactivation experiments were performed by exposing the plates to white LED light (75 W, 1800 lm, Satco) for 6 h. The light dose was 59.37 J/cm^2, and the light was approximately 35 cm away from the plate. Singlet oxygen detection experiments were performed using the same light 27 cm away from the 24-well plate, and the light doses were measured as 411.3, 822.6, 1645.2, 3290.4, 4935.6, 8226.0, and 39 484.8 J/cm^2 across the plate for the time points of 15 min, 30 min, 1 h, 2 h, 3 h, 5 h, and 24 h, respectively. The light dose was measured using a PASCO light sensor.

4.3. Cross-Linking Porphyrin 1 to Circular and Square PET Coupons. The combined mass of all the coupons was measured at each step to estimate the mass of cross-linked porphyrin on each coupon. A batch of 16 PET coupons (circular or square) were cleaned by submerging them in

https://doi.org/10.1021/acsomega.2c04294
ACS Omega 2022, 7, 29517−29525

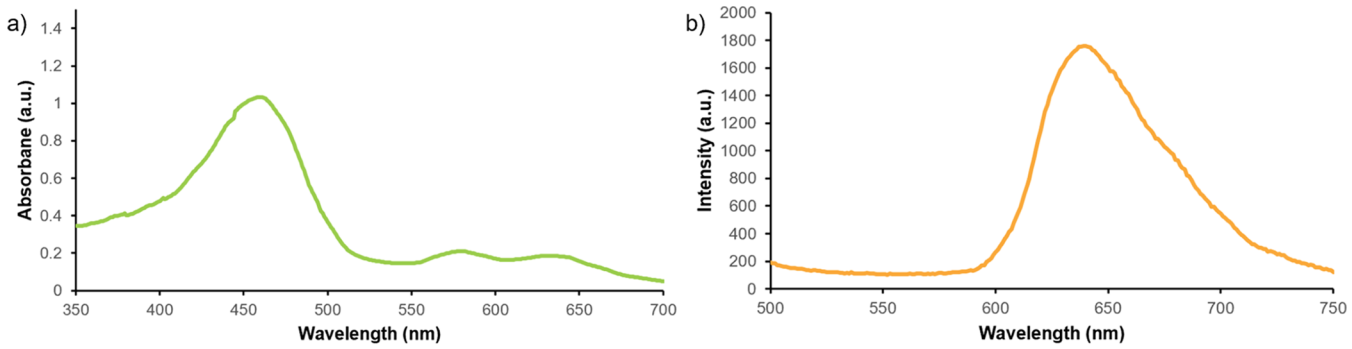

Figure 7. (a) UV−visible spectrum of porphyrin-functionalized PET. The maximum absorbance wavelength was determined to be λ_{max} = 459 nm. (b) Fluorescence emission spectrum of the porphyrin-functionalized PET. The maximum emission wavelength was determined to be λ_{em} = 640 nm.

methanol for at least 5 min and wiped with Kimwipes before being placed in an oven at 120 °C for 20 min to ensure they were dry. A solution of **1** and methanol was prepared (10 mg/mL). A spin-coater (MTI; VTC-50A) was used to spin-cast a 20 μL aliquot of the porphyrin solution onto each PET coupon at a speed of 10 000 rpm for 30 s. The coupons were allowed to air-dry for at least 20 min before they were placed in the oven at 120 °C for 18−24 h to allow the cross-linking reaction to take place. Excess **1** was removed from the coupons by rinsing them with methanol and wiping them with Kimwipes. The coupons were dried in the oven at 120 °C for at least 20 min. The coupons were kept in aluminum foil as much as possible throughout the process and stored in the dark until they were used during experiments to control and be consistent with the amount of light the coupons were exposed to. If a double-coated coupon was required, the procedure was repeated, and the masses were added at the end to determine the approximate amount on each coupon. Each single-coated circular coupon had ∼0.43 mg of porphyrin **1** for antimicrobial experiments (section 4.7) and ∼0.12 mg of porphyrin **1** for singlet oxygen detection (Section 4.5). Each square coupon had ∼0.32 mg of porphyrin **1**. The method used to determine the amount of porphyrin on each coupon can be found in Supporting Information.

4.4. Cross-Linking Control Experiment. For the control experiment, eight circular PET coupons were used. As seen in Figure 2, the coupons in row A had no treatment, the coupons in row B were treated with porphyrin **2** (containing no diazirine groups capable of engaging in C−H insertion) and 120 °C heat, the coupons in row C was spin coated with **1** without heating, and the coupons in row D were treated as described in section 4.3. The photograph in Figure 2 was captured after half of the coupons were rinsed after 24 h under the indicated conditions. Further characterization of the functionalized PET can be found in the Supporting Information.

4.5. Characterization of PET Coupons. Characterization of the PET coupons included absorption spectrscopy (Figure 7a), fluorescence emission spectroscopy (Figure 7b), infrared (IR) spectroscopy (Figure S4), and scanning electron microscopy (SEM) (Figure S5).[26] The coupons were prepared as described in section 4.3.

4.6. Singlet Oxygen Detection. Two stock solutions were prepared for the experiment. Circular coupons cross-linked with **1**, as described in section 4.3, had an average amount of ∼0.12 mg of **1** per coupon. One stock solution was PBS buffer, and the other stock solution was 0.18 mg/mL ADMA in PBS; sonication was used to ensure that the ADMA was fully dissolved. Two 24-well plates were used for each assay; one plate was wrapped in aluminum foil and reacted in the absence of light, and the other plate reacted in the light, as described in section 4.2.

Counting back from 24 h such that all experiments finished at the same time, a porphyrin−functionalized PET coupon was added to one well on each plate, and a blank circular coupon was added to another. To each well were added 200 μL of PBS and 200 μL of the ADMA solution for a total of 400 μL of solution in each well. The time points were set up as follows: 24 h, 5 h, 3 h, 2 h, 1 h, 30 min, 15 min, and 0 min. At the end of the assay, 100 μL aliquots of each sample were transferred to 96-well plates. Absorbance measurements were taken in the range of 300−500 nm using a Biotek Cytation 5 instrument. The experiment was performed in triplicate.

4.7. Antimicrobial Photodynamic Inactivation of *S. aureus*. *S. aureus* subsp. *aureus* (ATCC 6538P) was kindly provided by the Department of Biochemistry and Microbiology at University of Victoria. The strains were preserved in glycerol stocks (15%) and stored at −80 °C. Unless otherwise indicated, an overnight seed culture of *S. aureus*, cultured in LB broth, was diluted 1000-fold, which resulted in a bacterial suspension with a concentration of ∼10^5 CFU/mL. The standardized suspensions were used in the photoinactivation assays. The photoinactivation assays were performed as previously reported with minor modifications.[57,59]

The antibacterial effect of the cross-linked porphyrin was determined quantitatively by performing cell counts. PET coupons, which were modified as described in Section 4.3, were added to the bottom of wells in each of two 24-well microtiter plates (MTP), soaked in 96% ethanol, and left to dry under aseptic conditions. The wells were inoculated with 400 μL of the standardized bacterial suspension. One "light" plate was irradiated as mentioned in the previous section, and the other "dark" plate was wrapped with aluminum foil. In the absence of the cross-linked porphyrin, the effect of light was determined by inoculating unmodified wells on each plate with bacterial cells. After irradiation, the content of each well was serially diluted and plated on TSA. The colony-forming units were counted after overnight incubation. The experiment included two wells and was performed in triplicate. The results were calculated as the logarithmic reduction of the bacterial count (CFU/mL).

The qualitative determination of the porphyrin-functionalized circular coupons was performed by inoculating two TSA agar plates with 100 μL of the prepared bacterial suspension

https://doi.org/10.1021/acsomega.2c04294
ACS Omega 2022, 7, 29517−29525

using a sterile L-rod. Cross-linked porphyrin coupons and non-cross-linked sterile (PET) coupons (prepared as described in section 4.3) were placed on each inoculated TSA plate. The functionalized side was in direct contact with the inoculated agar plate surface. One plate was irradiated as mentioned in the previous section, while the other plate was wrapped with aluminum foil. After irradiation, the coupons were removed, and the plates were incubated at 37 °C. The antibacterial effect of the cross-linked porphyrin was determined after overnight incubation by checking for the presence of bacterial cells beneath the coupons.

■ ASSOCIATED CONTENT

Supporting Information

The Supporting Information is available free of charge at https://pubs.acs.org/doi/10.1021/acsomega.2c04294.

Synthesis of porphyrin **1**, synthesis of porphyrin **2**, infrared (IR) spectrum of porphyrin-functionalized PET, scanning electron microscope (SEM) image of porphyrin-functionalized PET, and method of determining amount of porphyrin PET coupons (PDF)

■ AUTHOR INFORMATION

Corresponding Author

Heather L. Buckley − *Department of Chemistry, Department of Civil Engineering, Centre for Advanced Materials and Related Technologies (CAMTEC), and Institute for Integrated Energy Systems (IESVic), University of Victoria, Victoria, BC V8P 5C2, Canada;* orcid.org/0000-0001-7147-0980; Email: hbuckley@uvic.ca

Authors

Stefania F. Musolino − *Department of Chemistry and Centre for Advanced Materials and Related Technologies (CAMTEC), University of Victoria, Victoria, BC V8P 5C2, Canada;* orcid.org/0000-0002-0990-1855

Fatima Shatila − *Department of Civil Engineering and Centre for Advanced Materials and Related Technologies (CAMTEC), University of Victoria, Victoria, BC V8P 5C2, Canada*

Grace M.O. Tieman − *Department of Chemistry, Centre for Advanced Materials and Related Technologies (CAMTEC), and Institute for Integrated Energy Systems (IESVic), University of Victoria, Victoria, BC V8P 5C2, Canada*

Anna C. Masarsky − *Department of Civil Engineering and Centre for Advanced Materials and Related Technologies (CAMTEC), University of Victoria, Victoria, BC V8P 5C2, Canada*

Matthew C. Thibodeau − *Department of Civil Engineering and Centre for Advanced Materials and Related Technologies (CAMTEC), University of Victoria, Victoria, BC V8P 5C2, Canada*

Jeremy E. Wulff − *Department of Chemistry and Centre for Advanced Materials and Related Technologies (CAMTEC), University of Victoria, Victoria, BC V8P 5C2, Canada;* orcid.org/0000-0001-9670-160X

Complete contact information is available at: https://pubs.acs.org/10.1021/acsomega.2c04294

Author Contributions

#S.F.M., F.S., and G.M.O.T. contributed equally. S.F.M. synthesized and characterized compounds **1** and **2**. F.S. designed and performed antimicrobial assays, with help from A.C.M. and M.C.T. G.M.O.T. designed and performed the singlet oxygen detection experiment. Cross-linking experiments were carried out by G.M.O.T., with help from F.S. H.L.B. and J.E.W. conceived the project and acquired funding to support the study. The manuscript was written through contributions of all authors. All authors have given approval to the final version of the manuscript.

Funding

We gratefully acknowledge Mitacs Canada (grant IT17318) and our industry partners, Epic Ventures, for fellowships and consumables support to S.F.M., F.S., G.M.O.T., A.C.M., and M.C.T. We also are grateful for the support from the IESVic Clean Energy Systems Accelerator Program (IESVic-CESAP) IRAP, NSERC USRA, Electricity Human Resources, EcoCanada, Biotalent Canada, and the UN Association of Canada.

Notes

The authors declare the following competing financial interest(s): H.L.B., J.E.W., and S.F.M. are co-authors on a patent (WO/2021/179064) that claims the use of compound **1** as a light-activated pathogen-killing molecule. There are no additional conflicts.

■ ACKNOWLEDGMENTS

The authors thank the department of microbiology and biochemistry for providing the *S. aureus* strain and Rebecca Hof and Dr. Joanne Hobbs for training and support.

■ ABBREVIATIONS

PET, polyethylene terephthalate; PBS, phosphate-buffer saline; ADMA, 9,10-anthracenediylbis(methylene)dimalonic acid; MTP, microtiter plates; HAI, hospital-acquired infections; LB, Luria−Bertani broth; TSA, tryptone soya agar.

■ REFERENCES

(1) Mahira, S.; Jain, A.; Khan, W.; Domb, A. J. Antimicrobial Materials—An Overview. In *Antimicrobial Materials for Biomedical Applications*; Domb, A. J., Kunduru, K. R., Farah, S., Eds.; Royal Society of Chemistry: Cambridge, UK, 2019; pp 1−37. DOI: 10.1039/9781788012638-00001.

(2) Li, X. F.; Mitch, W. A. Drinking Water Disinfection Byproducts (DBPs) and Human Health Effects: Multidisciplinary Challenges and Opportunities. *Environ. Sci. Technol.* **2018**, *52* (4), 1681−1689.

(3) Mith, H.; Duré, R.; Delcenserie, V.; Zhiri, A.; Daube, G.; Clinquart, A. Antimicrobial Activities of Commercial Essential Oils and Their Components against Food-borne Pathogens and Food Spoilage Bacteria. *Food Sci. Nutr.* **2014**, *2* (4), 403−416.

(4) Jones, A.; Mandal, A.; Sharma, S. Protein-Based Bioplastics and Their Antibacterial Potential. *J. Appl. Polym. Sci.* **2015**, *132* (18), 41931.

(5) Koshani, R.; Zhang, J.; van de Ven, T. G. M.; Lu, X.; Wang, Y. Modified Hairy Nanocrystalline Cellulose as Photobactericidal Nanofillers for Food Packaging Application. *ACS Sustainable Chem. Eng.* **2021**, *9* (31), 10513−10523.

(6) Chu, W.; Fang, C.; Deng, Y.; Xu, Z. Intensified Disinfection Amid COVID-19 Pandemic Poses Potential Risks to Water Quality and Safety. *Environ. Sci. Technol.* **2021**, *55* (7), 4084−4086.

(7) Jin, M.; Liu, L.; Wang, D.-n.; Yang, D.; Liu, W.-l.; Yin, J.; Yang, Z.-w.; Wang, H.-r.; Qiu, Z.-g.; Shen, Z.-q.; Shi, D.-y.; Li, H.-b.; Guo, J.-h.; Li, J.-w. Chlorine Disinfection Promotes the Exchange of Antibiotic Resistance Genes across Bacterial Genera by Natural Transformation. *ISME J.* **2020**, *14* (7), 1847−1856.

(8) *Tackling Drug Resistant Infections Globally: Final Report and Recommendations*; Review on Antimicrobial Resistance: London, England, 2016.

(9) Akarsu, E.; Uslu, R. Light-Activated Hybrid Organic/Inorganic Antimicrobial Coatings. *J. Sol-Gel Sci. Technol.* **2018**, *87* (1), 183−194.
(10) Hashempour-Baltork, F.; Hosseini, H.; Shojaee-Aliabadi, S.; Torbati, M.; Alizadeh, A. M.; Alizadeh, M. Drug Resistance and the Prevention Strategies in Food Borne Bacteria: An Update Review. *Adv. Pharm. Bull.* **2019**, *9* (3), 335−347.
(11) Gendron, F.; Nilson, S.; Ziffle, V.; Johnny, S.; Louie, D.; Diamente, P. Antimicrobial Effectiveness on Selected Bacterial Species and Alkaloid and Saponin Content of Rosa Nutkana C. Presl (Nootka Rose) and Urtica Dioica L. (Stinging Nettle) Extracts. *Am. J. of Plant Sci.* **2021**, *12* (05), 720−733.
(12) Sautrot-Ba, P.; Contreras, A.; Abbad Andaloussi, S.; Coradin, T.; Hélary, C.; Razza, N.; Sangermano, M.; Mazeran, P. E.; Malval, J. P.; Versace, D. L. Eosin-Mediated Synthesis of Polymer Coatings Combining Photodynamic Inactivation and Antimicrobial Properties. *J. Mater. Chem. B* **2017**, *5* (36), 7572−7582.
(13) Xu, G.; Neoh, K. G.; Kang, E. T.; Teo, S. L. M. Switchable Antimicrobial and Antifouling Coatings from Tannic Acid-Scaffolded Binary Polymer Brushes. *ACS Sustainable Chem. Eng.* **2020**, *8* (6), 2586−2595.
(14) Ghilini, F.; Pissinis, D. E.; Miñán, A.; Schilardi, P. L.; Diaz, C. How Functionalized Surfaces Can Inhibit Bacterial Adhesion and Viability. *ACS Biomater. Sci. Eng.* **2019**, *5* (10), 4920−4936.
(15) Mesquita, M. Q.; Dias, C. J.; Neves, M. G. P. M. S.; Almeida, A.; Faustino, M. A. F. Revisiting Current Photoactive Materials for Antimicrobial Photodynamic Therapy. *Molecules* **2018**, *23* (10), 2424.
(16) Valkov, A.; Nakonechny, F.; Nisnevitch, M. Polymer-Immobilized Photosensitizers for Continuous Eradication of Bacteria. *Int. J. Mol. Sci.* **2014**, *15* (9), 14984−14996.
(17) Nakonechny, F.; Barel, M.; David, A.; Koretz, S.; Litvak, B.; Ragozin, E.; Etinger, A.; Livne, O.; Pinhasi, Y.; Gellerman, G.; Nisnevitch, M. Dark Antibacterial Activity of Rose Bengal. *Int. J. Mol. Sci.* **2019**, *20*, 3196.
(18) Martínez, S. R.; Palacios, Y. B.; Heredia, D. A.; Aiassa, V.; Bartolilla, A.; Durantini, A. M. Self-Sterilizing 3D-Printed Polylactic Acid Surfaces Coated with a BODIPY Photosensitizer. *ACS Appl. Mater. Interfaces* **2021**, *13* (10), 11597−11608.
(19) Peveler, W. J.; Noimark, S.; Al-Azawi, H.; Hwang, G. B.; Crick, C. R.; Allan, E.; Edel, J. B.; Ivanov, A. P.; MacRobert, A. J.; Parkin, I. P. Covalently Attached Antimicrobial Surfaces Using BODIPY: Improving Efficiency and Effectiveness. *ACS Appl. Mater. Interfaces* **2018**, *10*, 98−104.
(20) Peddinti, B. S. T.; Morales-Gagnon, N.; Pourdeyhimi, B.; Scholle, F.; Spontak, R. J.; Ghiladi, R. A. Photodynamic Coatings on Polymer Microfibers for Pathogen Inactivation: Effects of Application Method and Composition. *ACS Appl. Mater. Interfaces* **2021**, *13*, 155−163.
(21) Felgenträger, A.; Maisch, T.; Späth, A.; Schröder, J. A.; Bäumler, W. Singlet Oxygen Generation in Porphyrin-Doped Polymeric Surface Coating Enables Antimicrobial Effects on Staphylococcus Aureus. *Phys. Chem. Chem. Phys.* **2014**, *16* (38), 20598−20607.
(22) Heredia, D. A.; Martínez, S. R.; Durantini, A. M.; Pérez, M. E.; Mangione, M. I.; Durantini, J. E.; Gervaldo, M. A.; Otero, L. A.; Durantini, E. N. Antimicrobial Photodynamic Polymeric Films Bearing Biscarbazol Triphenylamine End-Capped Dendrimeric Zn(II) Porphyrin. *ACS Appl. Mater. Interfaces* **2019**, *11* (31), 27574−27587.
(23) Baigorria, E.; Durantini, J. E.; Martínez, S. R.; Milanesio, M. E.; Palacios, Y. B.; Durantini, A. M. Potentiation Effect of Iodine Species on the Antimicrobial Capability of Surfaces Coated with Electroactive Phthalocyanines. *ACS Appl. Bio Mater.* **2021**, *4* (12), 8559−8570.
(24) Spagnul, C.; Turner, L. C.; Giuntini, F.; Greenman, J.; Boyle, R. W. Synthesis and Bactericidal Properties of Porphyrins Immobilized in a Polyacrylamide Support: Influence of Metal Complexation on Photoactivity. *J. Mater. Chem. B* **2017**, *5* (9), 1834−1845.
(25) Pereira, M. A.; Faustino, M. A. F.; Tomé, J. P. C.; Neves, M. G. P. M. S.; Tomé, A. C.; Cavaleiro, J. A. S.; Cunha, Â.; Almeida, A. Influence of External Bacterial Structures on the Efficiency of Photodynamic Inactivation by a Cationic Porphyrin. *Photochem. Photobiol. Sci.* **2014**, *13* (4), 680−690.
(26) Peddinti, B. S. T.; Scholle, F.; Ghiladi, R. A.; Spontak, R. J. Photodynamic Polymers as Comprehensive Anti-Infective Materials: Staying Ahead of a Growing Global Threat. *ACS Appl. Mater. Interfaces* **2018**, *10* (31), 25955−25959.
(27) Rapacka-Zdonczyk, A.; Wozniak, A.; Pieranski, M.; Woziwodzka, A.; Bielawski, K. P.; Grinholc, M. Development of Staphylococcus Aureus Tolerance to Antimicrobial Photodynamic Inactivation and Antimicrobial Blue Light upon Sub-Lethal Treatment. *Sci. Rep.* **2019**, *9*, 9423.
(28) Kashef, N.; Hamblin, M. R. Can Microbial Cells Develop Resistance to Oxidative Stress in Antimicrobial Photodynamic Inactivation? *Drug Resistance Updates* **2017**, *31*, 31−42.
(29) Cieplik, F.; Deng, D.; Crielaard, W.; Buchalla, W.; Hellwig, E.; Al-Ahmad, A.; Maisch, T. Antimicrobial Photodynamic Therapy−What We Know and What We Don't. *Crit. Rev. Microbiol.* **2018**, *44* (5), 571−589.
(30) Hu, X.; Huang, Y. Y.; Wang, Y.; Wang, X.; Hamblin, M. R. Antimicrobial Photodynamic Therapy to Control Clinically Relevant Biofilm Infections. *Front. Microbiol.* **2018**, *9*, 1299.
(31) Ozkan, E.; Allan, E.; Parkin, I. P. White-Light-Activated Antibacterial Surfaces Generated by Synergy between Zinc Oxide Nanoparticles and Crystal Violet. *ACS Omega* **2018**, *3* (3), 3190−3199.
(32) Alves, E.; Costa, L.; Carvalho, C. M.; Tomé, J. P.; Faustino, M. A.; Neves, M. G.; Tomé, A. C.; Cavaleiro, J. A.; Cunha, Â.; Almeida, A. Charge Effect on the Photoinactivation of Gram-Negative and Gram-Positive Bacteria by Cationic Meso-Substituted Porphyrins. *BMC Microbiol.* **2009**, *9*, 70.
(33) Hurst, A. N.; Scarbrough, B.; Saleh, R.; Hovey, J.; Ari, F.; Goyal, S.; Chi, R. J.; Troutman, J. M.; Vivero-Escoto, J. L. Influence of Cationic Meso-Substituted Porphyrins on the Antimicrobial Photodynamic Efficacy and Cell Membrane Interaction in Escherichia Coli. *Int. J. Mol. Sci.* **2019**, *20*, 134.
(34) Silveira, C. H. da; Vieceli, V.; Clerici, D. J.; Santos, R. C. V.; Iglesias, B. A. Investigation of Isomeric Tetra-Cationic Porphyrin Activity with Peripheral [Pd(Bpy)Cl]+ Units by Antimicrobial Photodynamic Therapy. *Photodiagn. Photodyn. Ther.* **2020**, *31*, No. 101920.
(35) Moreira, X.; Santos, P.; Faustino, M. A. F.; Raposo, M. M. M.; Costa, S. P. G.; Moura, N. M. M.; Gomes, A. T. P. C.; Almeida, A.; Neves, M. G. P. M. S. An Insight into the Synthesis of Cationic Porphyrin-Imidazole Derivatives and Their Photodynamic Inactivation Efficiency against Escherichia Coli. *Dyes Pigm.* **2020**, *178*, No. 108330.
(36) Prasanth, C. S.; Karunakaran, S. C.; Paul, A. K.; Kussovski, V.; Mantareva, V.; Ramaiah, D.; Selvaraj, L.; Angelov, I.; Avramov, L.; Nandakumar, K.; Subhash, N. Antimicrobial Photodynamic Efficiency of Novel Cationic Porphyrins towards Periodontal Gram-Positive and Gram-Negative Pathogenic Bacteria. *Photochem. Photobiol.* **2014**, *90* (3), 628−640.
(37) Mbakidi, J. P.; Herke, K.; Alvès, S.; Chaleix, V.; Granet, R.; Krausz, P.; Leroy-Lhez, S.; Ouk, T. S.; Sol, V. Synthesis and Photobiocidal Properties of Cationic Porphyrin-Grafted Paper. *Carbohydr. Polym.* **2013**, *91*, 333−338.
(38) Voit, T.; Cieplik, F.; Regensburger, J.; Hiller, K. A.; Gollmer, A.; Buchalla, W.; Maisch, T. Spatial Distribution of a Porphyrin-Based Photosensitizer Reveals Mechanism of Photodynamic Inactivation of Candida Albicans. *Front. Med.* **2021**, *8*, No. 641244.
(39) Nyga, A.; Czerwińska-Główka, D.; Krzywiecki, M.; Przystaś, W.; Zabłocka-Godlewska, E.; Student, S.; Kwoka, M.; Data, P.; Blacha-Grzechnik, A. Covalent Immobilization of Organic Photosensitizers on the Glass Surface: Toward the Formation of the Light-Activated Antimicrobial Nanocoating. *Materials* **2021**, *14* (11), 3093.
(40) Hwang, G. B.; Huang, H.; Wu, G.; Shin, J.; Kafizas, A.; Karu, K.; Toit, H. du; Alotaibi, A. M.; Mohammad-Hadi, L.; Allan, E.; MacRobert, A. J.; Gavriilidis, A.; Parkin, I. P. Photobactericidal

https://doi.org/10.1021/acsomega.2c04294
ACS Omega 2022, 7, 29517−29525

Activity Activated by Thiolated Gold Nanoclusters at Low Flux Levels of White Light. *Nat. Commun.* **2020**, *11*, 1207.
(41) Brovko, L.; Anany, H.; Bayoumi, M.; Giang, K.; Kunkel, E.; Lim, E.; Naboka, O.; Rahman, S.; Li, J.; Filipe, C. D. M.; Griffiths, M. W. Antimicrobial Light-Activated Materials: Towards Application for Food and Environmental Safety. *J. Appl. Microbiol.* **2014**, *117* (5), 1260−1266.
(42) Wright, T.; Vlok, M.; Shapira, T.; Olmstead, A. D.; Jean, F.; Wolf, M. O. Photodynamic and Contact Killing Polymeric Fabric Coating for Bacteria and SARS-CoV-2. *ACS Appl. Mater. Interfaces* **2022**, *14* (1), 49−56.
(43) Lepage, M. L.; Simhadri, C.; Liu, C.; Takaffoli, M.; Bi, L.; Crawford, B.; Milani, A. S.; Wulff, J. E. A Broadly Applicable Cross-Linker for Aliphatic Polymers Containing C-H Bonds. *Science* **2019**, *366*, 875−878.
(44) Musolino, S. F.; Pei, Z.; Bi, L.; DiLabio, G. A.; Wulff, J. E. Structure-Function Relationships in Aryl Diazirines Reveal Optimal Design Features to Maximize C-H Insertion. *Chem. Sci.* **2021**, *12* (36), 12138−12148.
(45) Cuthbert, T. J.; Ennis, S.; Musolino, S. F.; Buckley, H. L.; Niikura, M.; Wulff, J. E.; Menon, C. Covalent Functionalization of Polypropylene Filters with Diazirine−Photosensitizer Conjugates Producing Visible Light Driven Virus Inactivating Materials. *Sci. Rep.* **2021**, *11*, 19029.
(46) Polyethylene Terephthalate. *ChemicalBook*. https://www.chemicalbook.com/ChemicalProductProperty_EN_CB6493400.htm (accessed 2021-12-09).
(47) Entradas, T.; Waldron, S.; Volk, M. The Detection Sensitivity of Commonly Used Singlet Oxygen Probes in Aqueous Environments. *J. Photochem. Photobiol., B* **2020**, *204*, No. 111787.
(48) Openda, Y. I.; Ngoy, B. P.; Muya, J. T.; Nyokong, T. Synthesis, Theoretical Calculations and Laser Flash Photolysis Studies of Selected Amphiphilic Porphyrin Derivatives Used as Biofilm Photodegradative Materials. *New J. Chem.* **2021**, *45* (37), 17320−17331.
(49) Bhunia, A. K. *Foodborne Microbial Pathogens: Mechanisms and Pathogenisis*; Springer, 2008.
(50) Deyno, S.; Fekadu, S.; Astatkie, A. Resistance of Staphylococcus Aureus to Antimicrobial Agents in Ethiopia: A Meta-Analysis. *Antimicrob. Resist. Infect. Control* **2017**, *6*, 85.
(51) Bozja, J.; Sherrill, J.; Michielsen, S.; Stojiljkovic, I. Porphyrin-Based, Light-Activated Antimicrobial Materials. *J. Polym. Sci., Part A: Polym. Chem.* **2003**, *41* (15), 2297−2303.
(52) Ringot, C.; Sol, V.; Granet, R.; Krausz, P. Porphyrin-Grafted Cellulose Fabric: New Photobactericidal Material Obtained by "Click-Chemistry" Reaction. *Mater. Lett.* **2009**, *63* (21), 1889−1891.
(53) Ringot, C.; Sol, V.; Barrière, M.; Saad, N.; Bressollier, P.; Granet, R.; Couleaud, P.; Frochot, C.; Krausz, P. Triazinyl Porphyrin-Based Photoactive Cotton Fabrics: Preparation, Characterization, and Antibacterial Activity. *Biomacromolecules* **2011**, *12* (5), 1716−1723.
(54) Mbakidi, J. P.; Herke, K.; Alvès, S.; Chaleix, V.; Granet, R.; Krausz, P.; Leroy-Lhez, S.; Ouk, T. S.; Sol, V. Synthesis and Photobiocidal Properties of Cationic Porphyrin-Grafted Paper. *Carbohydr. Polym.* **2013**, *91*, 333−338.
(55) Wilson, M. Light-Activated Antimicrobial Coating for the Continuous Disinfection of Surfaces. *Infect. Control Hosp. Epidemiol.* **2003**, *24* (10), 782−784.
(56) López-Carballo, G.; Hernández-Muñoz, P.; Gavara, R.; Ocio, M. J. Photoactivated Chlorophyllin-Based Gelatin Films and Coatings to Prevent Microbial Contamination of Food Products. *Int. J. Food Microbiol.* **2008**, *126*, 65−70.
(57) Aluigi, A.; Sotgiu, G.; Torreggiani, A.; Guerrini, A.; Orlandi, V. T.; Corticelli, F.; Varchi, G. Methylene Blue Doped Films of Wool Keratin with Antimicrobial Photodynamic Activity. *ACS Appl. Mater. Interfaces* **2015**, *7* (31), 17416−17424.
(58) Condat, M.; Mazeran, P. E.; Malval, J. P.; Lalevée, J.; Morlet-Savary, F.; Renard, E.; Langlois, V.; Abbad Andalloussi, S.; Versace, D. L. Photoinduced Curcumin Derivative-Coatings with Antibacterial Properties. *RSC Adv.* **2015**, *5* (104), 85214−85224.
(59) Merchán, M.; Ouk, T. S.; Kubát, P.; Lang, K.; Coelho, C.; Verney, V.; Commereuc, S.; Leroux, F.; Sol, V.; Taviot-Guého, C. Photostability and Photobactericidal Properties of Porphyrin-Layered Double Hydroxide-Polyurethane Composite Films. *J. Mater. Chem. B* **2013**, *1*, 2139−2146.

https://doi.org/10.1021/acsomega.2c04294
ACS Omega 2022, 7, 29517−29525